Chapter-4

STUDIES ON SPECTRAL CHARACTERIZATION, CRYSTAL STRUCTURE NUCLEASE ACTIVITY AND CYTOTOXICITY OF MONONUCLEAR COPPER(II) COMPLEXES FORMED WITH TRIDENTATE LIGANDS

Introduction

Tridentate Schiff-bases are very efficient in coordinating with metal ions which prefer square-planar or square-pyramidal based geometry. Such complexes are also important as models for copper proteins containing active metal sites [1-5]. A large number of mono and polynuclear complexes of monocondensed imino-Schiff bases have been reported (Chapter 2-section 2 i), but there are a few reports available in the literature on DNA binding and cleavage activities of such complexes [6]. In the light of the above, mononuclear copper(II) complexes with tridentate ligands viz., 2-[1-(Methylamino-ethylimino)-methyl]-phenol (SAMEN) which is derived from salicylaldehyde and N-methylethylenediamine, 2-[1-(propylamino-ethylimino)-methyl]-phenol (SAPEN) which is derived from salicylaldehyde and N-propylethylenediamine, 2-[1-(Methylamino-ethylimino)-ethyl]-phenol (HAPMEN) which is derived from 2-hydroxyacetophenone and and N-methylethylenediamine and 2-[1-(propylamino-ethylimino)-ethyl]-phenol (HAPPEN) which is derived from 2-hydroxyacetophenone and N-propylethylenediamine are synthesized. Copper(II) complexes of these ligands were characterized by physico-chemical techniques and spectral methods viz., IR, UV-visible and ESR spectroscopy. Structure of copper(II) complex with 2-[1-(methylamino-ethylimino)-ethyl]-phenol (HAPMEN) is determined by single crystal x-ray diffraction analysis. Binding interactions of metal complexes with calf-thymus DNA are carried out using absorption spectrophotometry. Cleavage activities of these complexes are investigated on a double stranded pBR plasmid DNA by using gel electrophoresis experiments in the absence and in the presence of an oxidant, a complexing agent, a free radical scavenger and a reducing agent.

As reported in Chapter-3 (Section 3 ii), the ligands SAMEN, SAPEN, HAPMEN and HAPPEN were obtained as viscous liquids. General structure of the ligands is shown below:

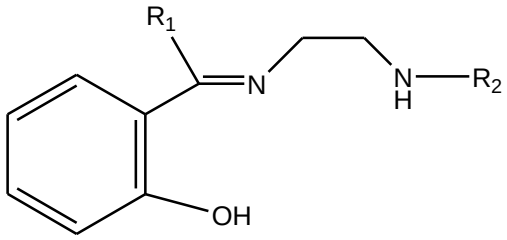

General structure of ligands

Ligand	R_1	R_2
SAMEN	H	CH_3
SAPEN	H	C_3H_7
HAPMEN	CH_3	CH_3
HAPPEN	CH_3	C_3H_7

Synthesis of metal complexes was given in Chapter-3 (Section 3 ii). All the complexes are stable at room temperature, non-hygroscopic, soluble in water, methanol, DMF and DMSO. Physical properties viz., colour of the complex, melting points and percentage of yield are given in **Table 4.1.**

i. Conductivity measurements

All the complexes are freely soluble in dimethylformamide (DMF), hence the solutions of these metal complexes were prepared in DMF to perform conductivity measurements. Milli-molar solutions (10^{-3}M) were prepared in 25- ml standard flask by dissolving the metal complex in DMF and then the solutions were transferred into a clean dry 100 ml beaker. Conductivity values of the solutions were measured at room temperature. Molar conductivity values of present copper(II) complexes suggest 1:1 electrolytic nature of the complexes [7]. The data are given in **Table 4.1.**

ii. Magnetic susceptibility measurements

Magnetic susceptibility values of all the complexes were measured at 298 K, using a magnetic susceptibility balance (Sherwood Scientific, Cambridge, UK). High purity copper sulfate pentahydrate was used as standard. Magnetic moments of copper(II) complexes were calculated using the following equations:

$$\chi_g = \left[\frac{C \times L \times (R^1 - R)}{m \times 10^9}\right] \longrightarrow 1$$

$$\chi_m = \chi_g \times (\text{molecular weight of the sample}) \longrightarrow 2$$

$$\mu_{eff} = 2.83 \sqrt{\chi_M T} \longrightarrow 3$$

Where

C = calibration constant

L = length of the sample taken in sample holder

R^1= Reading with sample

R = Reading without sample

m = weight of the sample taken in sample holder

T = Room temperature = 298 K

Calibration constant can be calculated using standard substance i.e. pentahydrated copper sulfate (χ_g = 5.92 × 10^{-6} cgs units). Magnetic susceptibility values of all the complexes are determined at room temperature in solid state. The magnetic moment values of copper complexes are found to be almost equal to spin only value. The values are found to be in the range of 1.84 to 1.96 BM which indicate the presence of unpaired electron. The data reveal that these complexes are monomeric and there is no metal-metal interaction [8]. The magnetic susceptibility data are shown in **Table 4.1.**

Table 4.2.1

Analytical and Physico-chemical properties of copper (II) complexes

Complex	Colour (Yield %)	Decoposition temp. °C	Magnetic moment μ_{eff} (BM)	Molar conductivity ($\Omega^{-1}cm^2mol^{-1}$)	Elemental Analysis*			
					C%	H%	N%	Cu%
$[Cu(SAMEN)(H_2O)_2]NO_3$	Dark green (69)	274-276	1.86	62	35.42 (35.45)	5.09 (5.06)	12.42 (12.48)	18.68 (18.76)
$[Cu\ (SAPEN)\ (H_2O)_2]NO_3$	Dark green (59)	268-270	1.78	58	39.22 (39.29)	5.79 (5.77)	11.43 (11.45)	17.34 (17.32)
$[Cu(HAPMEN)(H_2O)_2]NO_3$	Dark green (62)	278-280	1.90	63	37.49 (37.45)	5.42 (5.43)	11.96 11.91)	17.87 (18.01)
$[Cu(HAPPEN)\ (H_2O)_2]NO_3$	Dark green (64)	265-267	1.84	69	40.92 (40.99)	6.01 (6.09)	11.07 (11.03)	16.76 (16.68)

*Calculated values are given in parentheses.

iii. Electronic spectra

Transition metal complexes exhibit various colours due to the redistribution of electrons in the partially filled d-orbitals and referred as d-d transitions. In absence of the ligands around the metal, the energy, of all five d-orbitals of a transition metal ion are equal and are degenerate. The presence of ligands will result in splitting in the energy levels of these orbitals. In metal complexes some orbitals will interact more strongly than others. The exact form of interaction and energies of d-orbitals depend on the arrangement of ligands around the metal ion. In UV-visible, near IR region of electromagnetic radiation, the transition associated with electronic energy levels of the compound under investigation can be identified. The electronic spectral data of copper(II) complexes are recorded in water and in dimethylformamide (DMF). Typical electronic spectrum of $[Cu(SAMEN)(H_2O)_2]NO_3$ is shown in **Fig 4.1.** In aqueous solution all the complexes show strong intense bands in the region 37878-38461 cm^{-1} (λ = 260 – 264 nm) attributed due to intraligand and π-π^* aromatic ring and imine moiety, one medium intensity band observed in the region 27244-27984 cm^{-1} (λ = 345 – 366 nm) is due to metal to ligand charge transfer transition (MLCT). Whereas one broad band observed in the region 16320-16891 cm^{-1} (λ = 592 – 606 nm) is assigned to d-d transitions in favour of square pyramidal geometry around Cu(II) atom [9-11]. In DMF the absorption bands are shifted to higher wavelengths (bathochromic shift, $\Delta\lambda$ = 9 – 14 nm) suggesting the involvement of solvent molecules in coordination. Absorption bands with comparable features have been previously assigned to copper(II) complexes having square pyramidal structure with considerable distortion towards trigonal bipyramidal structure [12]. Important electronic spectral bands of copper(II) complexes are shown in **Table 4.2.**

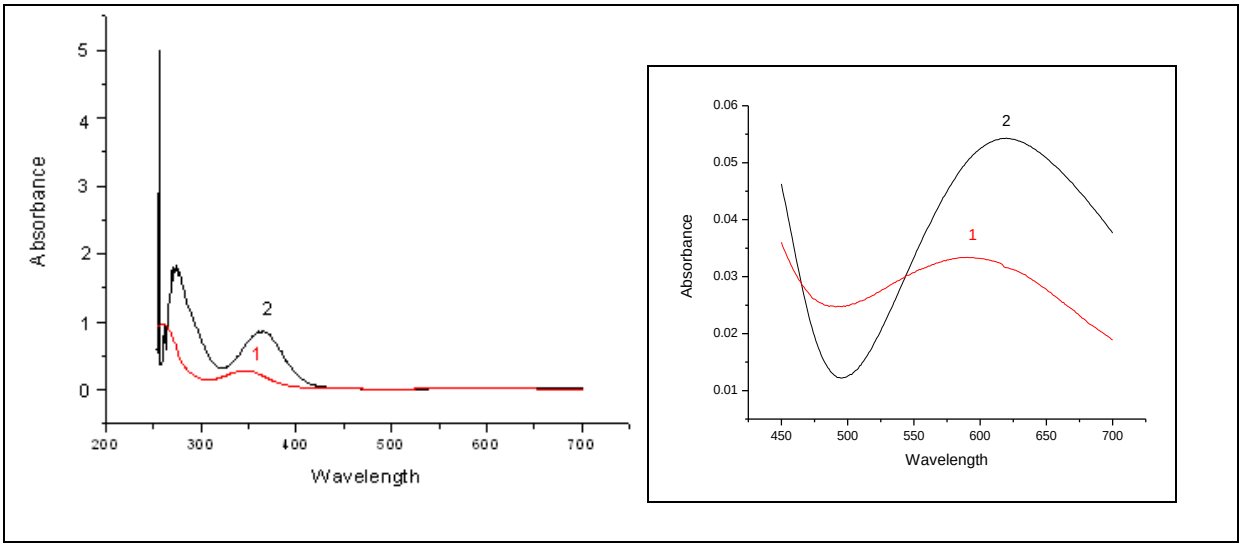

Fig 4.1: Electronic spectrum of [Cu (SAMEN) $(H_2O)_2$]NO_3 (1) in H_2O and (2) in DMF; Spectrum of highly concentrated (1 x 10^{-3} M) solution is given in the inset.

Table 4.2: Electronic spectral data (cm^{-1}) of copper (II) complexes

Complex	$\pi - \pi^*$		Charge transfer (CT)		d – d	
	H_2O	DMF	H_2O	DMF	H_2O	DMF
[Cu (SAMEN)$(H_2O)_2$]NO_3	37878 (264)	36496 (274)	28328 (353)	27700 (361)	16320 (606)	16130 (620)
[Cu (SAPEN)$(H_2O)_2$]NO_3	38022 (263)	36549 (273)	28818 (347)	27862 (359)	16722 (598)	16452 (607)
[Cu (HAPMEN)$(H_2O)_2$]NO_3	38461 (260)	37548 (266)	28985 (345)	27984 (357)	16778 (596)	16500 (606)
[Cu (HAPPEN)$(H_2O)_2$]NO_3	38461 (260)	37336 (267)	27322 (366)	27244 (367)	16891 (592)	16548 (604)

Wavelengths (λ) in nm are shown in parantheses
Approximate ε values are: $\pi - \pi^*$ ~ 440, CT ~ 210, d – d ~ 40 lit mol^{-1} cm^{-1}

iv. Infrared spectra

In the infrared spectra of the present copper(II) complexes an absorption band is observed in the region 3100-3200 cm^{-1}, which is assigned to ν(OH) of the coordinated water molecules. A weak medium band observed in the region 3416-3454 cm^{-1} is assigned to secondary N-H group. The absorption bands in the range 1610-1635 cm^{-1} are assigned to the coordinated azomethine (C=N) group. The bands observed at 1360–1338 cm^{-1} are due to the non-coordinated nitrate present in the complexes [13]. If the nitrate group is coordinated, then the peak might have been present in the region 1260-1285 cm^{-1} [13]. IR spectral data of the complexes are presented in Table 4.3. Typical IR spectrum of [Cu (SAPEN) $(H_2O)_2]NO_3$ is shown in Fig 4.2.

Table 4.3: Important IR spectral bands of complexes

Complex	ν (H_2O) cm^{-1}	ν (N-H) cm^{-1}	ν (Ring C-H) cm^{-1}	ν (C=N) cm^{-1}	ν (NO_3) cm^{-1}	ν (M-O) cm^{-1}	ν (M-N) cm^{-1}
$[Cu(SAMEN)(H_2O)_2]NO_3$	3416	3100	2900	1635	1347	514	442
$[Cu(SAPEN)(H_2O)_2]NO_3$	3454	3200	2924	1633	1354	521	498
$[Cu(HAPMEN)(H_2O)_2]NO_3$	3443	3188	2910	1625	1338	528	457
$[Cu(HAPPEN)(H_2O)_2]NO_3$	3428	3154	2934	1610	1360	506	435

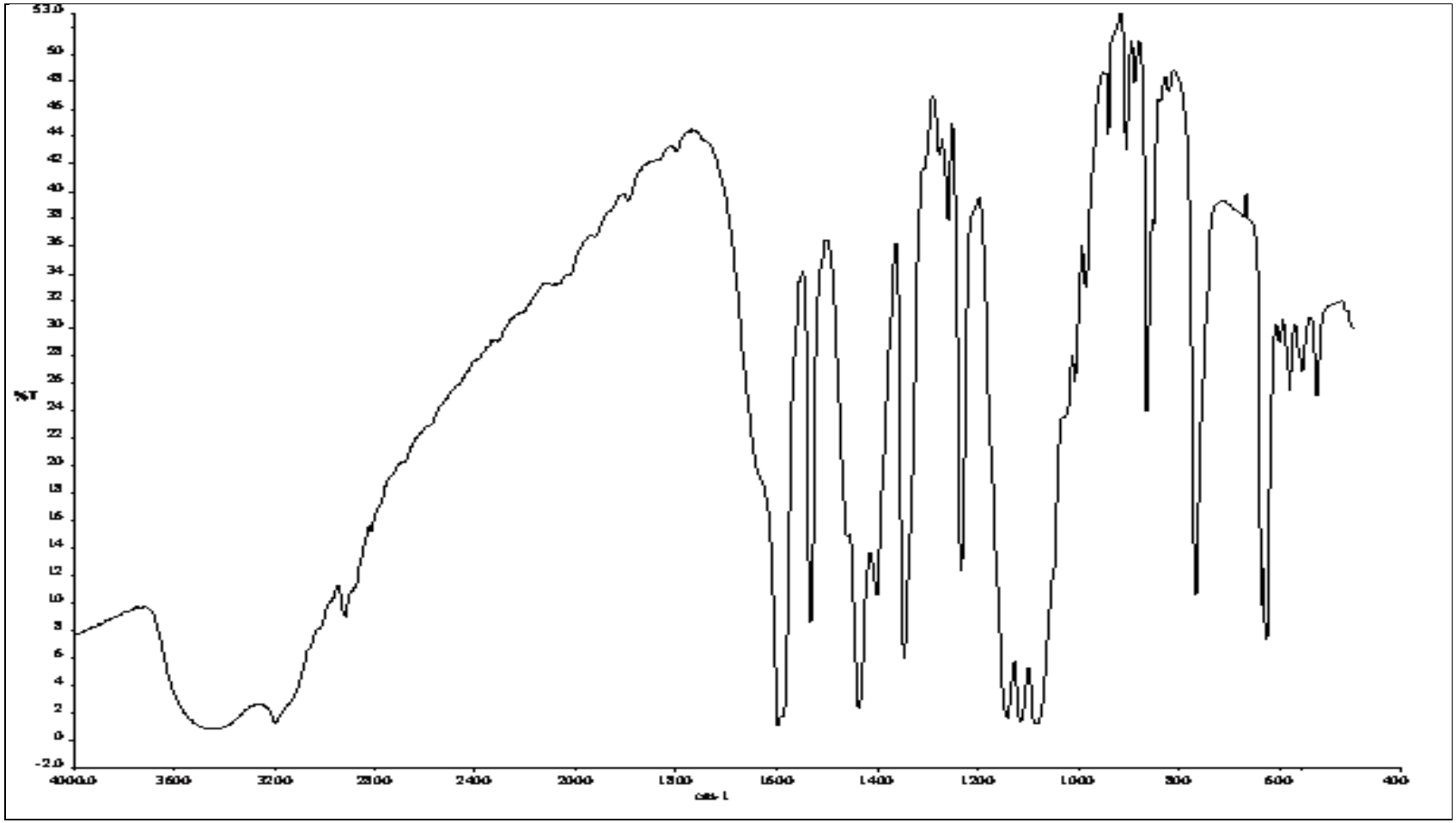

Fig 4.2: FT-IR spectrum of [Cu (SAPEN) $(H_2O)_2$]NO_3

v. ESR spectral studies

The copper(II) ion has an effective spin of S = ½ and associated with angular momentum (ms = ±1/2) leading to a doubly degenerate spin state in the absence of a magnetic field. In a magnetic field, this degeneracy is removed and the energy difference between these two states is given by $E= h\nu = g\beta H$

Where h = Plank's constant

ν = the frequency of radiation used

g = The Lande's splitting factor equal to 2.00277 for the free electron

β = Electronic Bohr magneton and

H = Strength of applied magnetic field.

For normal field strength (ca. 3500 gauss), the resonance frequency is 10^4 MHz (X-band microwave region) and hence for the free copper (II) ion there is also an interaction with the magnetic field due to the orbital angular momentum (L) of the electron. Hence, the total interaction becomes E = (2.0023+S+L) H.

The orbital degeneracy is removed by the crystal field and the orbital angular momentum is said to be quenched for the ground states of copper (II) complexes. The spin orbit coupling mixes into the ground state and some orbital angular momentum from certain excited state leading to the modifications in the Lande's splitting factor (g).

In the octahedral case, the *g* factor is isotropic and increased above the free ion value (2.003) by the factor $6 \lambda r^2/\Delta$ where Δ is the crystal field splitting energy, λ is spin orbital coupling constant (equal to -0.83KK) and *r* measures the combined reduction of the orbital coupling constant from their free ion values to those in the actual complexes. It is influenced by the factors such as covalent bonding and electron delocalization from the ligand atom to the copper(II) ion. In axial copper (II) ion environment the *g* factors are anisotropic (g_z = g

and g_x, g_y = g) as the effect of mixing in is no longer isotropic. The expressions for the *g* values of a copper (II) ion in different ligand fields are summarized.

1. **Cubic**

$$g_\perp = 2 - \left(\frac{4r^2\lambda}{\Sigma d_{xy}, d_{xz}, d_{yz} \rightarrow d_{x^2-y^2}, d_{z^2}} \right)$$

2. **Axial**

   a. **Elongated –$d_{x^2-y^2}$ (or d_{xy}) ground state**

$$g_\perp = 2 - \left(\frac{2r^2\lambda}{\sum d_{xz}, d_{yz} \rightarrow d_{x^2-y^2},} \right)$$

$$g_\parallel = 2 - \left(\frac{8r^2\lambda}{\sum d_{xy} \rightarrow d_{x^2-y^2}} \right)$$

$$g_\parallel >> g_\perp > 2.0$$

   b. **Compressed –d_{z^2} ground state**

$$g_\perp = 2 - \left(\frac{6r^2\lambda}{\sum d_{x^2}, d_{y^2} \rightarrow d_{z^2}} \right)$$

$$g_\parallel = 2.0$$

$$g_\perp >> g_\parallel = 2.0$$

ESR spectra of copper complexes were recorded in Varian E-112 X-band spectrophotometer at room temperature and liquid nitrogen temperature (LNT) in both solution ((DMF) and solid state.

Typical X-band ESR spectra of [Cu(HAPMEN) $(H_2O)_2$]NO_3 complex is shown in **Fig 4.3**. The spin Hamiltonian and orbital reduction parameters of mononuclear complexes are given in **Table 4.4**. The $g_\parallel$ and $g_\perp$ values are computed from the spectrum using (TCNE) free radical as 'g' marker. From the observed values of complexes at 300K and 77K in solid state spectrum it is clear that $g_\parallel > g_\perp > 2.00$ which suggests the fact that the unpaired electrons lies

predominantly in the $d_{x^2-y^2}$ orbital [14] characteristic of square pyramidal geometry in copper(II) complexes [11]. For ESR spectra at 77 K and 300 K, the 'G' values are found to be more than 4, which suggests that there is no interaction between copper(II) ions in the solid state or in solution state.

The solution EPR spectra recorded in DMF, shows four-hyperfine signals which were not observed in DMF at 77 K. The spin-orbit coupling constant, λ value of the complexes calculated using the relations, $g_{av} = 1/3[g_{\parallel} + 2g_{\perp}]$ and $g_{av} = 2(1-2\lambda/10Dq)$, is less than the free Cu(II) ion (-832cm^{-1}) which also supports the covalent nature of M-L bond in the complexes [14]. Hathaway [14] has pointed out that for the pure σ – bonding $K_{\parallel} \approx K_{\perp} \approx 0.77$, for in-plane π-bonding $K_{\parallel} < K_{\perp}$, while for out-of-plane π-bonding $K_{\parallel} > K_{\perp}$. The observed $K_{\parallel} > K_{\perp}$ relation in all the complexes indicates the presence of out-of-plane π-bonding [15].

The greater value of $g_{\parallel}$ compared to $g_{\perp}$ proposes a distorted square pyramidal structure and rules out the possibility of a trigonal bipyramidal structure which is expected to have $g_{\perp} > g_{\parallel}$[16,17]. Also, the observed $g_{\parallel}$ values of less than 2.3 provide evidence for the covalent character of bonding between Cu(II) ion and the ligand [18]. Increasing steric hindrance caused by bulky ligands results in the lowest $A_{\parallel}$ and highest $g_{\parallel}$ values, which in turn reflects in square pyramidal distortion of copper(II) geometries. As the bulkiness increases, an increased distortion in square pyramidal structure is observed which is reflected in the values of $g_{\parallel}/ A_{\parallel}$ [19]. The in-plane bonding parameter α^2 values are calculated using the following relation:

$$\alpha^2 = - (A_{\parallel}/0.036) + (g_{\parallel} - 2.0023) + 3/7 (g_{\perp} - 2.0023) + 0.04.$$

As the square pyramidal distortion increases, there is a gradual decrease in the value of α^2 indicating that there is a substantial in-plane bonding in these complexes.

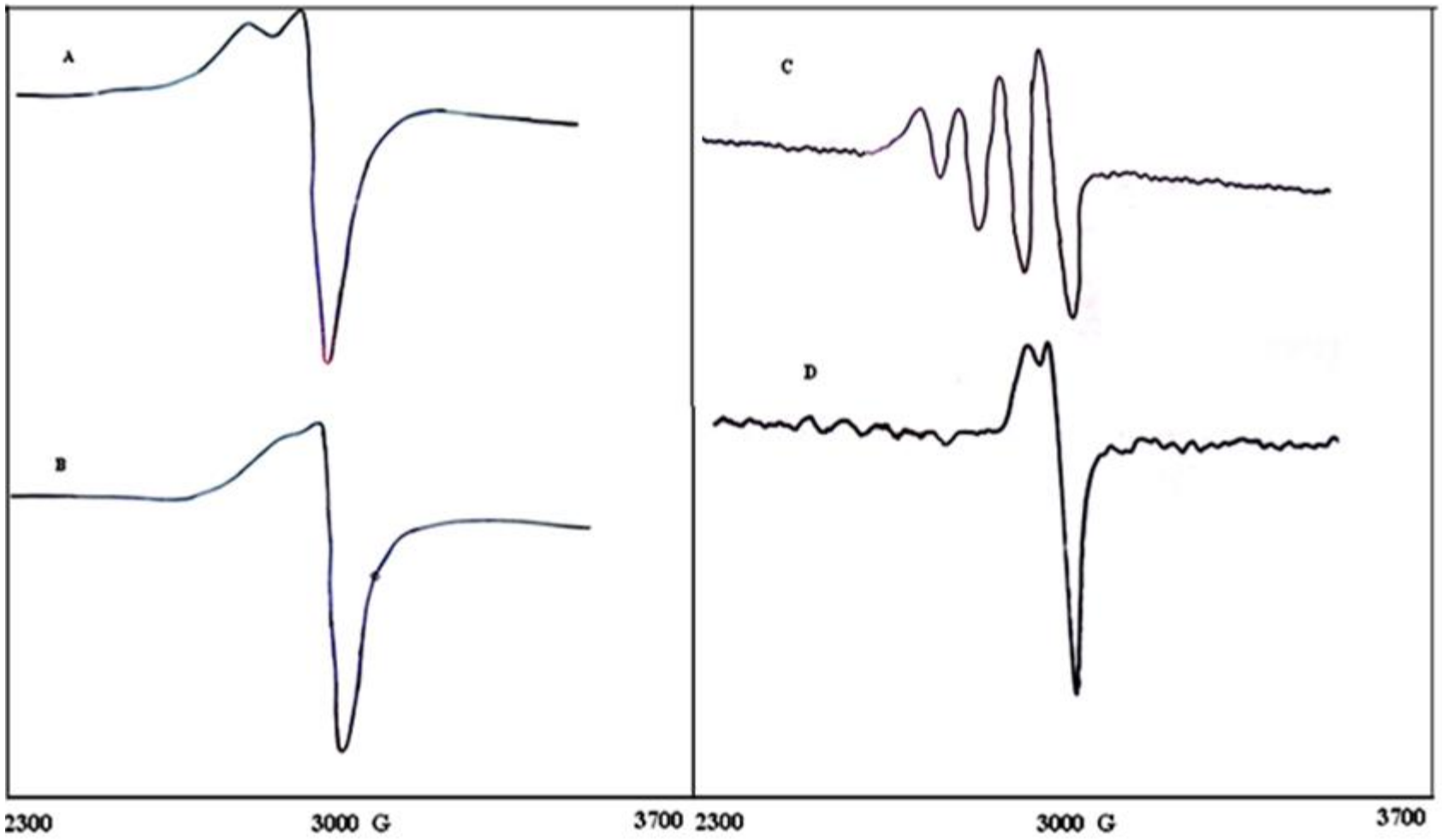

Fig 4.3: (A) X-band powder ESR spectra of $[Cu(HAPMEN(H_2O)_2]NO_3$ at 300K, (B) at LNT, (C) in DMF solution at 300K and (D) at LNT in DMF solution

Table 4.4:
Spin Hamiltonian and orbital reduction parameters for copper (II) complexes at 300 and 77 K in solid state and in DMF solution

Complex	In solid state				In DMF solution										
	$g_{\parallel}$	$g_{\perp}$	g_{av}	G	$g_{\parallel}$	$g_{\perp}$	g(av)	G	λ	$K_{\parallel}$	$K_{\perp}$	$A_{\parallel}$ cm^{-1}	$A_{\perp}$ cm^{-1}	A_{av}	$g_{\parallel}/A_{\parallel}$	α^2
$[Cu(SAMEN)(H_2O)_2]NO_3$	2.046	2.011	2.023	4.752	2.144	2.030	2.068	5.046	283	1.020	0.908	0.0105	0.0023	0.0050	204	0.097
$[Cu(SAPEN)(H_2O)_2]NO_3$	2.153	2.040	2.077	4.007	2.180	2.043	2.088	4.373	365	1.001	0.959	0.0103	0.0023	0.0049	211	0.052
$[Cu(HAPMEN)(H_2O)_2]NO_3$	2.207	2.021	2.040	4.117	2.197	2.050	2.099	4.098	408	0.991	0.980	0.0098	0.0017	0.0044	224	0.018
$[Cu(HAPPEN)\ (H_2O)_2]NO_3$	2.213	2.036	2.070	4.011	2.216	2.055	2.109	4.005	441	0.988	0.989	0.0096	0.0014	0.0041	230	0.010

Based on molar conductivity, magnetic moments, electronic and ESR spectral data, the complexes are found to be mononuclear and penta-coordinated. Square pyramidal geometry is assigned to all these complexes. Among the five coordinate sites of metal ion, three are occupied by N, N, O donor atoms of tridentate ligand. The remaining two sites are occupied by water molecules. Based on these observations the tentative structure of the complexes is given in **Fig 4.4.**

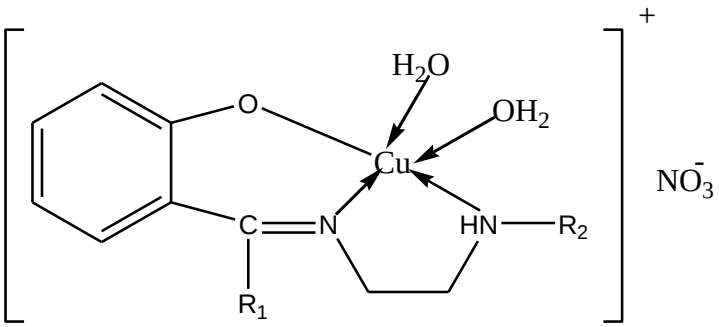

Where R_1 = H/CH_3 and R_2 = CH_3/C_3H_7

Fig 4.4: A general structure for metal complex

iv. Single crystal X-ray studies

Isolation of single crystals

The author has tried to isolate the single crystals of all the complexes. But only the complex $[Cu(HAPMEN)(H_2O)_2]NO_3$ is obtained as single crystals suitable for x-ray diffraction studies successfully. Deep green single crystals of complex were grown in methanol on slow diffusion with n-hexane.

Description of crystal structure of $[Cu(HAPMEN)(H_2O)_2]NO_3$

The complex crystallizes in monoclinic, space group $P2_1/n$ with the unit cell parameters; a=7.874(5) Å, b=20.908(4) Å, c=9.119(2) Å, $\alpha = \gamma = 90°$ and β=107.324(5), V=1433.2(10)$Å^3$, Z=4. Crystal data and structure refinements are given in **Table. 4.5.** The structure is shown in **Fig 4.5** together with the numbering scheme in the metal coordination sphere. The molecule contains a five coordinated Cu(II) atom, while the basal plane is occupied by three donor atoms O(1), N(1), N(2) of the tridentate ligand together with two oxygen atoms O(2) and O(3) of the coordinated water molecules. The axial Cu(1)–O(3) bond distance of 2.417(4) Å is larger than the basal Cu(1)–O(1) and Cu(1)–O(2) bond distances of 1.878(3)Å and 2.006(3) Å respectively. This indicates geometry around the Cu(II) atom is distorted square-pyramidal [20,21]. Close packing diagram of $[Cu(HAPMEN)(H_2O)_2]NO_3$ is shown in **Fig 4.6.** Geometric details describing the intermolecular O(3)–H(3A)$^{\cdots}$O(4) hydrogen bond in the complex: H(3A)$^{\cdots}$ 1.95(3) Å, O(3)$^{\cdots}$O(4)=2.812(6) Å with angle at H(2B) = 165(5). Intermolecular interactions operating in the crystal structure of $[Cu(HAPMEN)(H_2O)_2]NO_3$: O(2)–H(2B).....$O(3)^{\#1}$ = 2.14(4) Å; O(2)–O(3) = 2.871(5) Å with angle at H(2B) = 144(6) for symmetry operation #1 -x+2,-y,-z+3 ; O(3)–H(3B).....$O(1)^{\#1}$ = 1.98(4) Å; O(3)–O(1) = 2.808(5) Å with angle at H(2B) = 154(6)for symmetry operation #1 -x+2,-y,-z+3 and O(2)-H(2A)...$O(4)^{\#2}$ = 2.54(5) Å; O(2)$^{\cdots}$O(4) = 3.168(5) Å with angle at H(2)A=129(5)^o for #2 x+1,y,z. Hydrogen

bonding data are listed in **Table 4.4.** Crystal data and structure refinement are presented in **Table 4.5.** Selected bond lengths and bond angles are summarized in **Table 4.6** and **4.7** respectively.

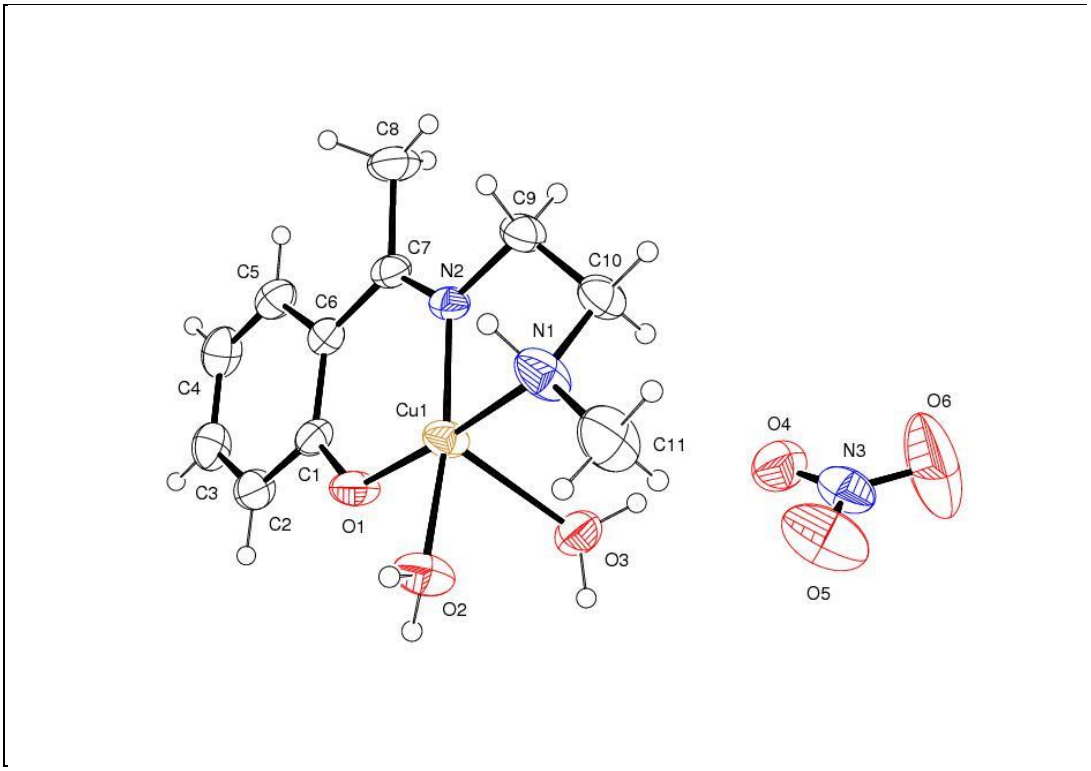

Fig 4.5: ORTEP view of $[Cu(HAPMEN)(H_2O)_2]NO_3$

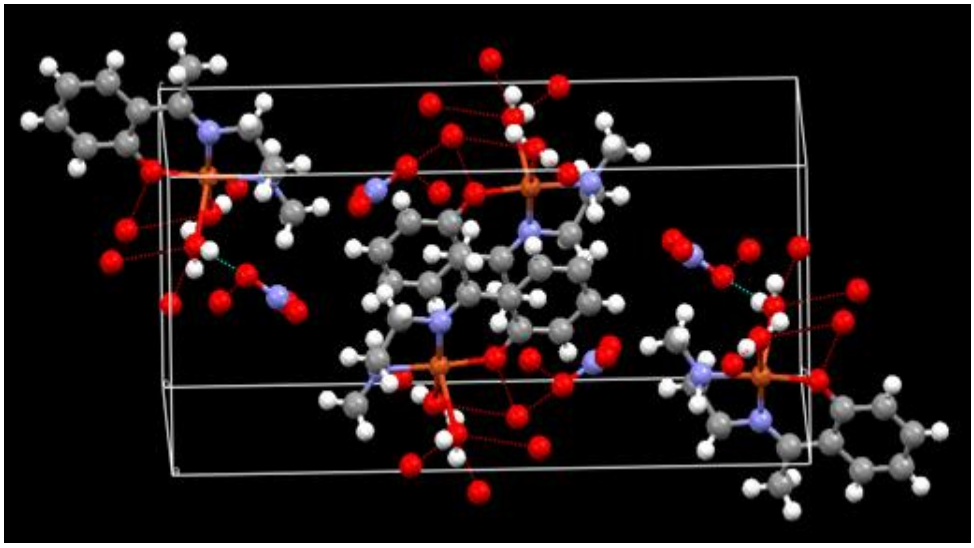

Fig 4.6: Close packing diagram of $[Cu(HAPMEN)(H_2O)_2]NO_3$

Table 4.4: Hydrogen bonds for [Cu(HAPMEN)(H_2O)$_2$]NO_3 [A° and °]

D-H...A	d(D-H)	d(H...A)	d(D...A)	<(DHA)
O(2)-H(2B)...O(3)#1	0.875(19)	2.12(4)	2.871(5)	144(6)
O(2)-H(2A)...O(4)#2	0.875(19)	2.54(5)	3.168(5)	129(5)
O(2)-H(2A)...O(4)#2	0.895(19)	1.92(3)	2.799(6)	165(5)
O(2)-H(2A)...O(6)#2	0.895(19)	2.47(5)	3.162(8)	135(5)
O(2)-H(2A)...N(3)#2	0.895(19)	2.54(3)	3.384(6)	157(6)
O(3)-H(3A)...O(4)	0.880(19)	1.95(3)	2.812(6)	165(5)
O(3)-H(3B)...O(1)#1	0.89(2)	1.98(3)	2.808(5)	154(6)

Symmetry transformations used to generate equivalent atoms:

#1 -x+2,-y,-z+3 #2 x+1,y,z

Table 4.5: Crystal data and structure refinement for [Cu(HAPMEN)(H_2O)$_2$]NO_3

Identification code	shelxl
Empirical formula	C_{11} H_{19} Cu N_3 O_6
Formula weight	352.83
Temperature	293(2) K
Wavelength (Mo Kα) (Å)	0.71073 A
Crystal system	Monoclinic
Space group	P21/n
Unit cell dimensions	
a (Å)	7.874(5)
b (Å)	20.908(4)
c(Å)	9.119(2)
α (^{o})	90(5)
β (^{o})	107.324(5)
γ (^{o})	90(5)
Volume V (A^3)	1433.2(10)
Z	4
Calculated density, ρ(Mg m^{-3})	1.635
Absorption coefficient μ(mm^{-1})	1.555

F(000)	732
Crystal size	0.30 X 0.20 X 0.20 mm
θ Range for data collection	2.53 - 24.99°
Limiting indices	$-9 \leq h \leq 9$, $-23 \leq k \leq 24$, $-10 \leq l \leq 10$
Reflections collected	13991
Unique reflections	2513 [R(int) = 0.0236]
Completeness to θ	24.99 99.8 %
Absorption correction	Semi-empirical from equivalents
Maximum and minimum transmission	0.7512 and 0.6462
Refinement Method	full-matrix least-squares on F^2
Data/restraints/parameters	2513 / 8 / 212
Goodness-of-fit on F^2	1.181
Final R indices [$I > 2\sigma(I)$]	[a]R_1 = 0.0465, [b,c] wR_2 = 0.1061
R indices (all data)	[a]R_1 = 0.0572, [b,c] wR_2 = 0.1362
Largest diff. peak and hole (e.Å^{-3})	0.685 and -0.400

[a] $R_1 = \sum(\left|F_O\right| - \left|F_C\right| / \sum \left|F_O\right|$. [b] $wR_2 = \{\sum [w (F_O^2 - F_C^2)^2] / \sum [w(F_O^2)^2]\}^{1/2}$

[c] $w = 1/[\sigma^2(F_O^2) + (aP)^2 + bP]$ with $P = [F_o^2 + 2F_c^2]/3$, a=0.0612 and b =0.24.

Table 4.6: Selected bond lengths [A°] for $[Cu(HAPMEN)(H_2O)_2]NO_3$

Atoms	Bond length
N(1)-Cu(1)	1.999(4)
N(1)-H(1)	0.97(2)
N(2)-Cu(1)	1.955(3)
N(3)-O(5)	1.178(6)
N(3)-O(6)	1.183(6)
N(3)-O(4)	1.241(6)
O(1)-Cu(1)	1.878(3)

O(2)-Cu(1)	2.006(3)
O(2)-H(2B)	0.875(19)
O(2)-H(2A)	0.895(19)
O(3)-Cu(1)	2.417(4)
O(3)-H(3A)	0.880(19)
O(3)-H(3B)	0.89(2)

Table 4.7: Selected bond angles [°] for [Cu(HAPMEN)(H_2O)$_2$]NO_3

Atoms	bond angles
C(11)-N(1)-Cu(1)	122.0(4)
C(10)-N(1)-Cu(1)	103.3(3)
C(7)-N(2)-Cu(1)	127.7(3)
C(9)-N(2)-Cu(1)	111.0(3)
C(1)-O(1)-Cu(1)	127.0(3)
Cu(1)-O(2)-H(2B)	118(4)
Cu(1)-O(2)-H(2A)	121(4)
Cu(1)-O(3)-H(3A)	118(4)
Cu(1)-O(3)-H(3B)	115(4)
O(1)-Cu(1)-N(2)	93.25(13)
O(1)-Cu(1)-N(1)	175.89(18)
N(2)-Cu(1)-N(1)	84.74(15)
O(1)-Cu(1)-O(2)	88.27(13)
N(2)-Cu(1)-O(2)	169.88(15)
N(1)-Cu(1)-O(2)	93.09(15)
O(1)-Cu(1)-O(3)	88.71(13)
N(2)-Cu(1)-O(3)	105.44(14)
N(1)-Cu(1)-O(3)	95.27(18)
O(2)-Cu(1)-O(3)	84.59(16)

The single crystal x-ray diffraction analysis confirms the structure suggested in **Fig 4.4** based on spectral analysis.

v. Cyclic voltammetric studies

Redox behavior of the copper(II) complexes have been investigated by cyclic voltammetry in DMF using 0.1M tetrabutylammoniumhexaflourophosphate (TBAHEP) as supporting electrolyte. The cyclic voltammetric profile of [Cu(HAPPEN) $(H_2O)_2$]NO_3 is given in **Fig 4.7**. The electrochemical data of copper(II) complexes are presented in **Table 4.9.**

Repeated scans at various scan rates suggest that the presence of stable redox species in solution. $E_{1/2}$ values of all complexes observed at potential range of 0.122 – 0.397 V vs. Ag/AgCl [22-24]. It may be inferred that all the Cu(II) complexes undergo reduction to their respective Cu(I) complexes. The non-equivalent current in cathodic and anodic peaks (i_c/i_a= 1.192 – 1.801 at 100 mVs^{-1}) for complexes indicate quasi-reversible behavior [25]. The difference $\Delta E_p = E_{pc} - E_{pa}$ in all the complexes exceeds the Nerstian requirement 59/n mV (n= number of electrons involved in oxidation reduction) which suggests quasi-reversible character associated with a considerable reorganization of the coordination sphere during electron transfer [26]. The complexes have large separation (154-550 mv) between anodic and cathodic peaks indicating quasi-reversible character. The $E_{1/2}$ values of copper complexes are inversely related to the size of the complex. As the molecular weight of the complex increases, the $E_{1/2}$ value decreases [27].

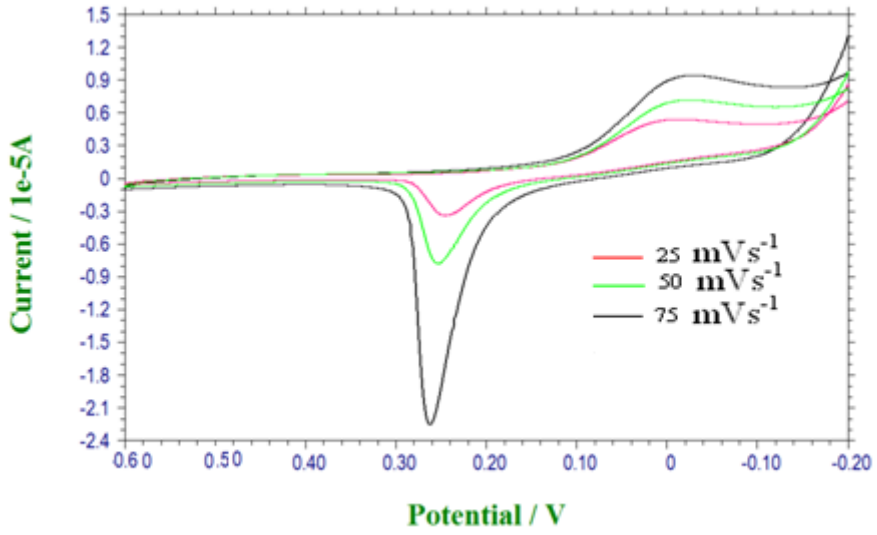

Fig 4.7: Cyclic voltammetric profile of $[Cu(HAPPEN)(H_2O)_2]NO_3$ at different scan rates 25, 50 and 75 mVs^{-1}

Table 4.9:
Cyclic voltammetric data of copper(II) complexes

Complex	Redox couple	E_{pc} V	E_{pa} V	ΔE_p (mV)	$E_{1/2}$	$-i_c/i_a$	log K_c [a]	$-\Delta G^o$ [b]
$[Cu(SAMEN)(H_2O)_2]NO_3$	II/I	0.268	0.526	258	0.397	1.268	0.130	747
$[Cu(SAPEN)(H_2O)_2]NO_3$	II/I	0.292	0.446	154	0.369	1.192	0.218	1251
$[Cu(HAPMEN)(H_2O)_2]NO_3$	II/I	-0.104	0.446	550	0.171	1.658	0.061	350
$[Cu(HAPPEN)(H_2O)_2]NO_3$	II/I	-0.020	0.265	285	0.122	1.801	0.117	672

[a] $\log K_c = 0.434\ ZF/RT\Delta E_p$; [b] $\Delta G^o = -2.303\ RT \log K_c$

viii. DNA binding studies of copper(II) complexes

The interaction of metal complexes was monitored by UV-visible spectroscopy. The absorption spectra of complexes were compared in the absence and in the presence of CT-DNA. In the presence of increasing amounts of DNA, the spectra of all complexes showed a strong decrease (Hypochromicity) or increase (Hyperchromicity) in intensity with shift in absorption maxima towards lower (blue-shift) or higher (red-shift) wave lengths. The change in absorbance values with increasing amount of CT-DNA were used to evaluate the intrinsic binding constant K_b for the complex.

Copper(II) complexes exhibit an intense absorption band around 332-366 nm which is attributed to metal-ligand charge transfer (MLCT) transitions. Absorption spectra were recorded in the range of 250-500 nm. Electronic absorption spectral data (upon addition of CT-DNA) and binding constants of these complexes are given in the **Table 4.10**. The change in absorbance values with increasing amounts of CT-DNA was used to evaluate the intrinsic binding constant K_b, for the complexes. In the presence of increasing amounts of CT-DNA, the UV-Visible absorption spectra of copper (II) complexes show bathochromic shift (λ_{max}: 1-15nm). It is evident from the table, that all the complexes bind with DNA with high affinities and, the estimated binding constants are in the range 8-9 x 10^6 M^{-1}. This may be due to the presence of pi- stacking of the phenyl ring present in the Schiff base ligand. Typical absorption spectra of $[Cu(SAPEN)(H_2O)_2]$ NO_3 in presence and in absence of DNA are shown in **Fig 4.13.**

The binding constants (K_b) for DNA interaction of the complexes have been calculated by using the following equation:

$$[DNA] / (\varepsilon_a-\varepsilon_f) = [DNA] / (\varepsilon_b-\varepsilon_f) + 1/ K_b (\varepsilon_b-\varepsilon_f) \qquad (1)$$

Table 4.10:

Electronic absorption data upon addition of CT-DNA to Cu(II) complexes

Complex	$\lambda_{max/nm}$		Δλ/nm	H%	$K_b(M^{-1})$
	Free	Bound			
$[Cu(SAMEN)(H_2O)_2]\ NO_3$	366	351	15	-16.07	9.91×10^6
$[Cu(SAPEN)(H_2O)_2]\ NO_3$	332	330	2	8.21	9.25×10^6
$[Cu(HAPMEN)(H_2O)_2]\ NO_3$	348	344	4	-9.64	8.68×10^6
$[Cu(HAPPEN)(H_2O)_2]\ NO_3$	341	342	1	6.23	8.36×10^6

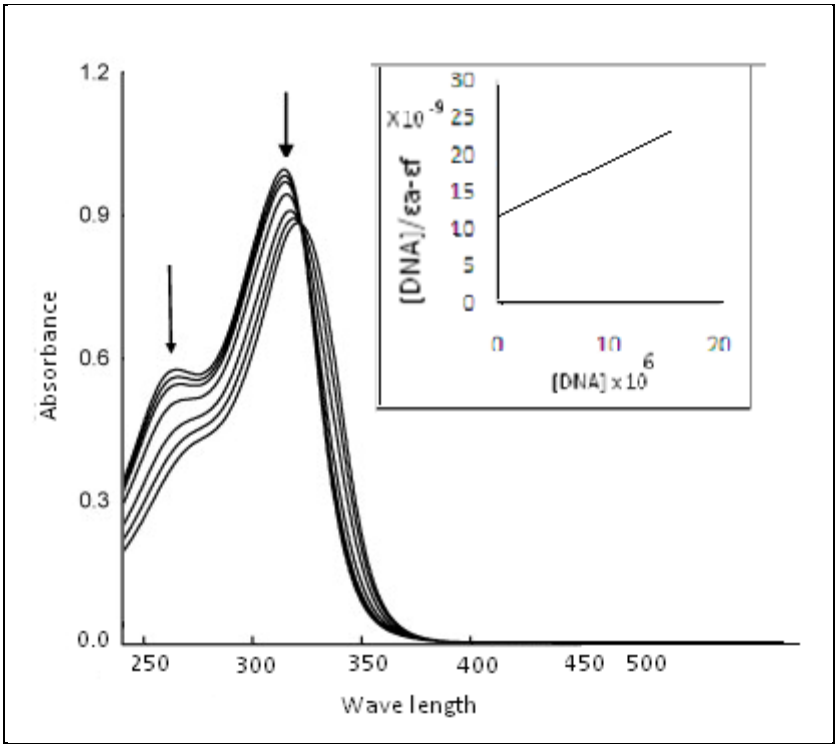

Fig 4.13: **Absorption spectra of $[Cu(SAPEN)(H_2O)_2]\ NO_3$ in the absence and in the presence of increasing concentration of CT-DNA; top most spectrum is recorded in the absence of DNA; A plot of [DNA]/(ε_a-ε_f) versus [DNA] is shown in the inset**

ix. DNA cleavage activities of copper(II) complexes

Nuclease activity of mono-nuclear copper(II) complexes derived from tridentate Schiff base ligands has been studied by agarose gel electrophoresis using pBR 322 plasmid DNA in Tris-HCl/NaCl (50mM / 5mM) buffer (pH-7) in the presence and absence of H_2O_2 after 30 minutes incubation period at 37°C[28,29]. Nuclease activity of complexes was also investigated in presence of free radical scavenger (DMSO), chelating agent (EDTA) and reducing agent DTT. In the absence of H_2O_2 the complexes cleaved supercoiled DNA (Form 1) into nicked DNA (Form II) (**Fig. 4.14** and **4.15**, lane 3 and 8). From **Fig 4.14** (lanes 4 & 9) and **Fig 4.15** (lanes 4 & 9) it is evident that copper complexes cleave DNA more effectively in the presence of oxidant which may be due to hydroxyl radical (OH) reaction with DNA. This is consistent with the increased production of hydroxyl radicals by cuprous ions similar to the well known Fenton reaction [30].

$$Cu(II) + H_2O_2 \rightleftharpoons Cu(I) + \dot{O}OH + H^+$$

$$Cu(I) + H_2O_2 \rightleftharpoons Cu(II) + \dot{O}H + {}^-OH$$

These hydroxyl radicals participate in the oxidation of the deoxyribose moiety, followed by hydrolytic cleavage of the sugar backbone [31]. The more pronounced nuclease activity of the complexes in the presence of oxidant indicates the participation of hydroxyl radical in DNA cleavage.

The nuclease activity of the copper complexes was also investigated in the presence of a free radical scavenger, dimethyl sulfoxide (DMSO), a chelating agent EDTA and a reducing agent dithiotreitol (DTT). In presence of DMSO cleavage activity of the complex $[Cu(SAMEN)(H_2O)_2]\ NO_3$ is less when compared with $[Cu(SAPEN)(H_2O)_2]\ NO_3$ according to the **Fig 4.14** (lanes 5 & 10). Chelating agent EDTA decreases the nuclease activity of copper complexes (lanes 6 & 11 of **Figures 4.14 & 4.15**), whereas in presence of reducing agent (DTT) the cleavage activity of copper complexes is enhanced. This may be due to formation of copper(I) complex by catalytic reduction (lanes 7 & 12 of **Figures 4.14 & 4.15**).

Fig 4.14: Agarose gel (0.8%) showing results of electrophoresis of 1µl of pBR 322 Plasmid DNA; 4µl of Tris-HCl/NaCl (50mM/5mM) buffer (pH-7); 2µl of complex in DMF($1x10^{-3}$M); 11µl of sterilized water; 2µl of H_2O_2 (total volume 20µl) were added, respectively, incubated at 37^0C (30 min);

Lane 1: DNA control; Lane 2: DNA control + H_2O_2; Lane 3: [Cu(SAMEN)$(H_2O)_2$] NO_3 + DNA; Lane 4: [Cu(SAMEN)$(H_2O)_2$] NO_3 + DNA+ H_2O_2; Lane 5: [Cu(SAMEN)$(H_2O)_2$]NO_3 + DNA+DMSO; Lane 6: [Cu(SAMEN)$(H_2O)_2$] NO_3 + DNA + EDTA; Lane 7: [Cu(SAMEN)$(H_2O)_2$] NO_3 + DNA+DTT; Lane 8: [Cu(SAPEN)$(H_2O)_2$] NO_3+ DNA; Lane 9: [Cu(SAPEN)$(H_2O)_2$] NO_3 + DNA+ H_2O_2; Lane 10: [Cu(SAPEN)$(H_2O)_2$] NO_3 + DNA+DMSO; Lane 11: [Cu(SAPEN)$(H_2O)_2$] NO_3 + DNA+ EDTA; Lane 12: [Cu(SAPEN)$(H_2O)_2$] NO_3 + DNA+DTT;

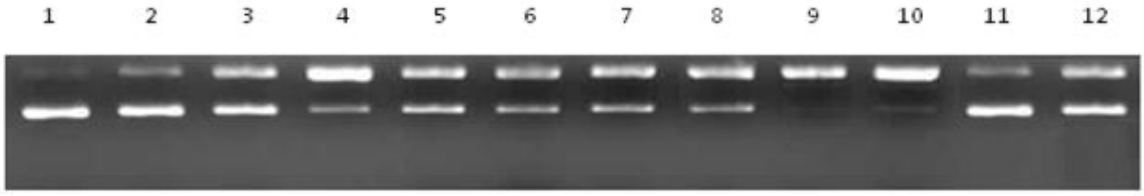

Fig 4.15: Agarose gel (0.8%) showing results of electrophoresis of 1µl of pBR 322 Plasmid DNA; 4µl of Tris-HCl/NaCl (50mM/5mM) buffer (pH-7); 2µl of complex in DMF($1x10^{-3}$M); 11µl of sterilized water; 2µl of H_2O_2 (total volume 20µl) were added, respectively, incubated at 37^0C (30 min);

Lane 1: DNA control; Lane 2: DNA control + H_2O_2; Lane 3: [Cu(HAPMEN)$(H_2O)_2$] NO_3 + DNA; Lane 4: [Cu(HAPMEN)$(H_2O)_2$] NO_3 + DNA+ H_2O_2; Lane 5: [Cu(HAPMEN)$(H_2O)_2$]NO_3 + DNA+DMSO; Lane 6: [Cu(HAPMEN)$(H_2O)_2$] NO_3 + DNA + EDTA; Lane 7: [Cu(HAPMEN)$(H_2O)_2$] NO_3 + DNA+DTT; Lane 8: [Cu(HAPPEN)$(H_2O)_2$] NO_3+ DNA; Lane 9: [Cu(HAPPEN)$(H_2O)_2$] NO_3 + DNA+ H_2O_2; Lane 10: [Cu(HAPPEN)$(H_2O)_2$] NO_3 + DNA+DMSO; Lane 11: [Cu(HAPPEN)$(H_2O)_2$] NO_3 + DNA+ EDTA; Lane 12: [Cu(HAPPEN)$(H_2O)_2$] NO_3 + DNA+DTT;

(x) Cytotoxic activity of copper(II) complexes

The MTT assay was done to check for the cytotoxic activity of the compounds on MCF-7 (a human breast carcinoma).

As all the present copper(II) complexes exhibit considerable DNA binding and cleavage activity, as most of the redox-active metal complexes showing DNA cleavage activity exhibit anticancer activity [32-37], the cytotoxicity of the complexes against the MCF-7 human breast cancer cell line was investigated by using MTT assay. The MTT Cell Proliferation and Viability Assay is a safe, sensitive, *in vitro* assay for the measurement of cell proliferation or, when metabolic events lead to apoptosis or necrosis, a reduction in cell viability. 5000 cells are plated in quadruplets at 100 μL/well for each variable in a 96-well tissue culture plates. Then the cells are treated with various concentrations of copper complexes after incubating at 37 °C for 16-18 h. 20 μL of MTT reagent (2.5 mg/ml) and 80 μl of medium are added to each well and further incubated for 2-4 hours at 37 °C [38]. When purple precipitate is clearly visible under the microscope, 100 μL of isopropanol is added to all wells, including control wells. The absorbance of the wells is measured at 570 nm, including the blank (100 μl isopropanol). A graph of absorbance versus treatment was plotted. The IC_{50} value defined [39] as the drug concentration that resulted in a 50% reduction in cell numbers compared to untreated controls was measured by plotting the percentage cytotoxicity versus concentration on a logarithmic graph by means of Eq. (1):

$$\% \text{ cell inhibition} = 100 - \text{Abs(sample)}/\text{Abs(control)} \times 100 \qquad (1)$$

The IC_{50} values obtained by plotting the cell viability against concentration of the complexes reveal that all of them exhibit least cytotoxicity after 24 h incubation. **Fig 4.16**

show the cytotoxic effect (% cell inhibition) of $[Cu(HAPMEN)(H_2O)_2]NO_3$. **Fig 4.17** displays the variation in the IC_{50} values of the complexes. **Table 4.11** gives the details of percentage of ratio of absorbance in sample well and absorbance in control well [Abs(sample)/Abs(control) × 100] and percentage of cell inhibition or viability. The calculated IC_{50} values are presented in **Table 4.12**. The values are in the range of 82.06 to 89.72 μM for all the complexes which reveal that the complexes are 6 times less cytotoxic than *cis*-platin. Among all the complexes $[Cu(SAMEN)(H_2O)_2]$ NO_3 shows the highest cytotoxicity. The data suggest that the cytotoxicity of the complexes is inversely proportional to their molecular weights. However the data reveal that cytotoxicity of the copper(II) complexes is not in good agreement with DNA binding and cleavage activity. This activity of the complexes thus suggests that *in vivo* mechanism of action of the complexes is more complicated than the one occurring for the *in vitro* DNA cleavage. The experiments indicate that cytotoxic effect of the present complexes was considerably less pronounced, since their IC_{50} values are sufficiently high.

Table 4.11:

***In vitro* cytotoxicity of the Cu(II) complexes in human breast (MCF7) cancer cell lines – Cell inhibition percentage**

Concentration	$[Cu(SAMEN)(H_2O)_2]NO_3$		$[Cu(SAPEN)(H_2O)_2]NO_3$		$[Cu(HAPMEN)(H_2O)_2]NO_3$		$[Cu(HAPPEN)(H_2O)_2]NO_3$	
	%OD	%IC	%OD	%IC	%OD	%IC	%OD	%IC
25 µg/ml	98.65	01.35	98.19	01.81	96.73	03.26	--	--
50 µg/ml	89.35	10.64	94.31	05.69	88.62	11.38	--	--
100 µg/ml	88.40	11.60	86.87	13.13	84.51	15.49	--	--

Table 4.12:

***In vitro* cytotoxicity of the Cu(II) complexes in human breast (MCF7) cancer cell lines – IC_{50} values of copper complexes**

Complex	**IC_{50} value (µM)**
$[Cu(SAMEN)(H_2O)_2]NO_3$(**1**)	82.06
$[Cu(SAPEN)(H_2O)_2]NO_3$ (**2**)	89.72
$[Cu(HAPMEN)(H_2O)_2]NO_3$(**3**)	86.60
$[Cu(HAPPEN)(H_2O)_2]NO_3$(**4**)	ND

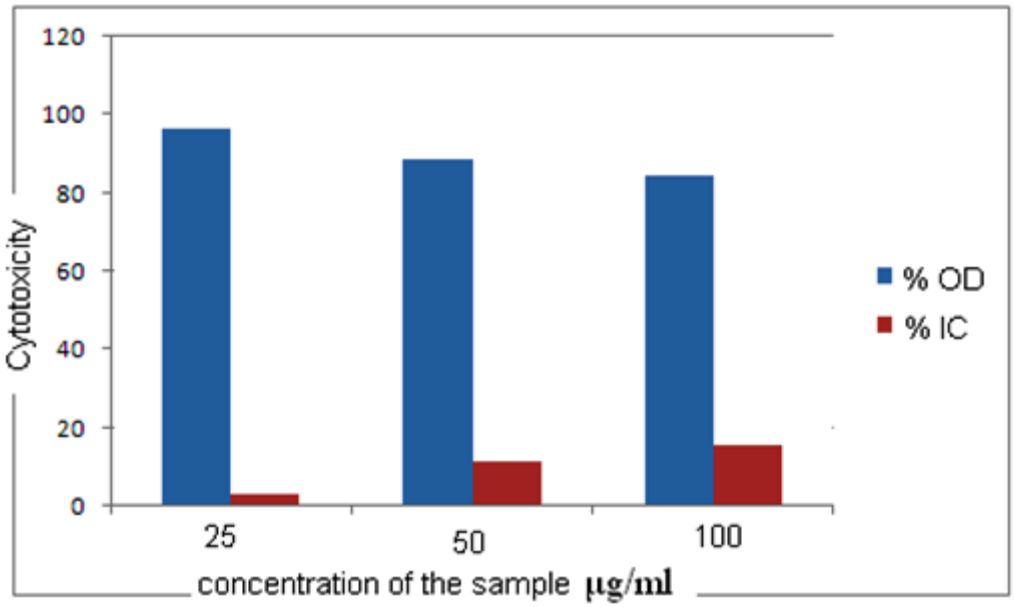

Fig 4.16: *In vitro* cytotoxicity of $[Cu(HAPMEN)(H_2O)_2]NO_3$ in human breast (MCF7) cancer cell lines – percentage of cell inhibition

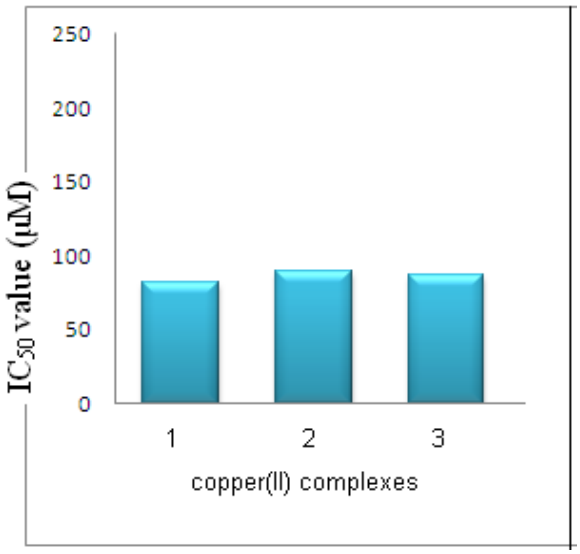

Fig 4.17: *In vitro* cytotoxicity of the Cu(II) complexes in human breast (MCF7) cancer cell lines - IC_{50} values of copper complexes

References:

1. E.Bouwman, W.L. Driessen, J. Reedijk, *Coord. Chem. Rev*., 104 (1990) 143.
2. K.D.Karlin, Z. Tyekla´r, *Adv. Inorg. Biochem*. 9 (1994) 123.
3. N. Kitajima, Y. Moro-oka, *Chem. Rev*. 94 (1994) 737.
4. E.I. Solomon, U.M. Sundaram, T.E. Machonkin, *Chem. Rev*. 96 (1996) 2563.
5. W.B. Tolman, *Acc. Chem. Res*. 30 (1997) 227.
6. P. Haribabu, *Ph.D., thesis*, Sri Krishnadevaraya University, Anantapur, Andhra Pradesh, 2011.
7. W. J. Geary, *Coord. Chem. Rev.* **7** (**1971)** 81.
8. S.Mandal and P.K.Bharadwaj, *Polyhedron*, 11 (**1992**), 1855.
9. Hathaway B.J., *comprehensive Coordination Chemistry*, Edited by G.Wilkinson, R.D. Gillard & J.A. Mecleverty (Pergfamon, Oxford), **1987**, Vol 5, p.583.
10. Patra A K, Ray M & Mukharjee R, *J Chem Soc, Dalton Trans*,(1999) 2461.
11. R.N.Patel, Nripendra Singh, D.K. Patel & V.L.N. Gundla, *Ind. J. Chem.*, 46A, **2007**, 422.
12. S.Bhattacharya, S.B.Kumar, S.K.Dutta, E.R.T.Tiekink and M.Chaudhury, *Inorg. Chem*, 35, **(1996),** 1967-73.
13. B. Keshavan, P.G. Chandrashekara, N.M. Made Gowda, *J. Mol. Struct.*, 553 (**2000**), 193.
14. B. Sarkar, M.S. Ray, Y.-Z Li, Y. Song, A. Figuerola, E. Ruiz, J. Cirera, J. Cano, A. Ghosh, *Chem. Eur. J.* 13 (**2007**) 9297.
15. B.J.Hathaway and D.E. Billing, *Coord. Chem. Rev.*, 5 **(1961)** 143.
16. S. Tyagi, B.J. Hathaway, *J. Chem. Soc. Dalton Trans.*, **1981**, 2029–2033.
17. E. Vi˜nuelas-Zahinos, M.A. Maldonado-Rogado, F. Luna-Giles, F.J. Barros-Garcia, *Polyhedron* 2008, **27**, 879–886
18. D. Kivelson, R. Neiman, *J. Chem. Phys.*, 1961,**35**,149–155.
19. Sagakuchi V & Addison A W, *J. Chem. Soc. Dalton Trans*., (**1979**) 600.
20. P.A.N. Reddy, M. Nethaji, A.R. Chakravarthy, *Eur. J. Inorg. Chem.* (**2003**), 2318.
21. V. Philip, V.Suni, M.R.P. Kurup, M. Nethaji, *Polyhedron*, 24 (**2005**) 1133.
22. X.H. Bu, Z.H. Zhang, X. Cao, S. Ma and Y. Tichen. *Polyhedron 16* (***1997***), p. *3525*.
23. S Dhar, D Senapathi, PK Das, P Chattopadyay, M Nethaji, AR Chakravarthy, *J Am.C*hem. *Soc **2003**, 125, 12218.*
24. Djebbar-Sid S, Benali-Baitich O and Deloume J P, *Polyhedron, 16**, 1997,** 2175*.

25. A.A.Khumhar, S.B.Rendye, D.X. West, A.E.Libert, *tran. Met. Chem.*. 16, **(1991),** 276.
26. S.Usha, M.Palaniandavar., *J. chem. Soc.*, *Dalton Trans*., (**1994**), 2277.
27. P.Muralikrishna, *Ph.D., thesis*, S.K.University, Anantapur, **2007.**
28. Murali Krishna P, Hussain Reddy K, Pandey JP, Dayananda S, *Trans. Met. Chem.* **(2008)** 33:661
29. P. Haribabu, Y. P. Patil, K Hussain Reddy, M. Nethaji, *Trans. Met. Chem.*36, 8 **(2011),** 867-874.
30. A.Hangan, A.Bodiki, L.Oprean, G.Alzuet, M.L. Gpnzalez, J.Borras., *Polyhedron*, 29, **2010,** 1305.
31. P.Merfey and E.R. Robinson, *Mutat. Res.*, 86 **(1981),** 155.
32. S. M. Cohen and S. J. Lippard, *Prog. Nucleic Acid Res. Mol. Biol*., 67 (**2001)** 93–130.
33. J. Wang, *Cell Death Differ*., 8 (**2001**) 1047–1048.
34. M. Valko, M. Izakovic, M. Mazur, C. J. Rhodes and J. Telser, *Mol.Cell. Biochem.*, 266 **(2004**) 37–56.
35. D. M. Perrin, A. Mazumder and D. S. Sigman, *Prog. Nucleic Acid Res. Mol. Biol.*, 52 (**1996**) 123–151.
36. A. J. Danford, D. Wang, Q. Wang, T. D. Tullius and S. J. Lippard, *Proc. Natl. Acad.Sci. U. S. A.*, 102 (**2005**) 12311–12316.
37. S. Bhattacharya and S. S. Mandal, *Chem. Commun.*, 13 (**1996**) 1515–1516.
38. T. Mosmann, J. Immunol. *Methods* 65 (**1983**) 55.
39. K.Abdi, H.Hadadzadeh,M.Weil, M.Salimi, *Polyhedron*, 31 (**2012**) 638–648.